Lifetimes and structure of excited states of ^{115}Sb

Yu. N. Lobach
Institute for Nuclear Research, pr. Nauki 47, 252028 Kiev, Ukraine

D. Bucurescu
Horia Hulubei Institute of Physics and Nuclear Engineering, 76900 Bucharest, Romania

(Received 7 October 1997)

Lifetimes of excited states of ^{115}Sb were measured by the Doppler shift attenuation method in the $(\alpha,2n\gamma)$ reaction at $E_\alpha = 27.2$ MeV. The experimental level scheme and the electromagnetic transition probabilities have been interpreted in terms of the interacting boson-fermion model. A reasonable agreement with the experiment was obtained for the positive-parity states. The experimental data also show the applicability of the cluster-vibrational model for the mixing of two $9/2^+$ states having different intrinsic configurations. [S0556-2813(98)07205-7]

PACS number(s): 21.10.Tg, 21.60.Fw, 23.20.Lv, 27.60.+j

I. INTRODUCTION

The level scheme of ^{115}Sb at low and medium excitation energies was previously investigated with the $(p,2n\gamma)$ [1], $(\alpha,2n\gamma)$ [2], and $(^6\mathrm{Li},3n\gamma)$ [3] reactions, respectively, as well as through the β decay of ^{115}Te [4]. Recently, the high-spin region of this nucleus was investigated using heavy-ion reactions [5,6]. As a result of these works a detailed level scheme has been obtained. Similarly to the other light odd antimony isotopes, the spectrum of the excited states of ^{115}Sb is determined by the valence proton beyond the $Z=50$ closed shell and its interaction with collective and quasiparticle excitations of the Sn core. Moreover, a striking peculiarity inherent to these isotopes are collective bands arising from the excitation of a $2p$-$1h$ proton state [7–11]. Such an interpretation has commonly been based on the level energies only, since the experimental data for electromagnetic transition probabilities is very poor and limited to three isomeric states of ^{115}Sb in the nanosecond region [2,3,12]. Lifetime measurements in the picosecond region for low-lying states in ^{115}Sb have been reported recently, with the use of the $(p,n\gamma)$ reaction [13]. The aim of the present work is a further study of the lifetimes of excited states in this nucleus, by the $(\alpha,2n\gamma)$ reaction, and an appropriate interpretation of the structure of this nucleus on the basis of current nuclear models.

II. EXPERIMENTAL PROCEDURE AND RESULTS

The lifetime experiment was performed at the U-120 cyclotron of the Institute for Nuclear Research in Kiev. A self-supported ^{113}In target of thickness 8.5 mg/cm^2 and 92% enrichment was used. The excited states of ^{115}Sb were populated in the reaction $^{113}\mathrm{In}(\alpha,2n\gamma)$ at a bombarding energy of 27.2 MeV. The initial recoil velocity of 0.54% of the velocity of light was determined from the reaction kinematics. A high purity Germanium detector of 40% relative efficiency and 2.2 keV full width at half maximum (FWHM) energy resolution at $E_\gamma = 1.3$ MeV was located at a distance of 17 cm from the target. The γ-ray spectra were measured at angles of 30°, 60°, 90°, 120°, and 150° with respect to the beam direction. Figure 1 shows the spectrum obtained at 90°; spectra with similar statistics were obtained at the other angles.

The lifetimes of the excited states were obtained from an analysis of the Doppler shift attenuated line shapes measured at different angles. Such an analysis was carried out using an updated version of the computer code described in Ref. [14]. For the slowing-down process Lindhard's cross sections [15] were used, with the correction factors $f_e=1.3$ and $f_n=0.9$ for the electronic and nuclear stopping power, respectively. These values are suggested from the analysis of the slowing-down process of Cd ions in a Cd target [16]. The velocity distribution of the emitting nuclei was calculated from the simulation of 30 000 recoil histories by a Monte Carlo code which takes into account reactions at different depths of the target, the kinematics of the reaction, as well as the slowing down and the deflection of the recoils. The components of the velocity distributions seen at each of the five detector angles were stored in ''shape-time'' matrices containing 20 time steps over the range 0.01–10.0 ps. Each matrix contains the complete spectrum of line shapes from fully shifted to

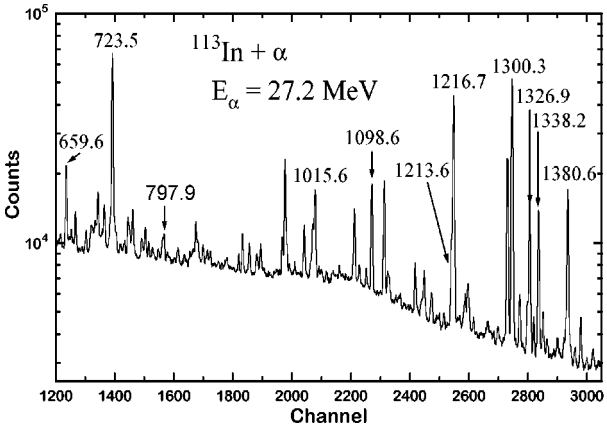

FIG. 1. Spectrum of the $^{113}\mathrm{In}(\alpha,2n\gamma)$ reaction at 27.2 MeV incident energy, measured at 90°. Some of the ^{115}Sb γ-ray transitions of interest are marked by their energies in keV (see also Fig. 2). All the other spectra (at 30°, 60°, 120°, and 150°) have been measured with similar statistical accuracy.

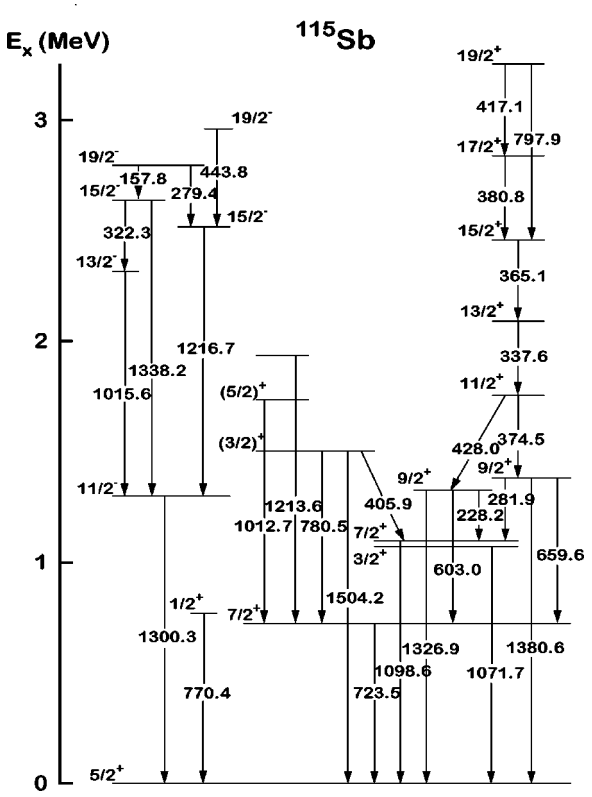

FIG. 2. Partial level scheme of ^{115}Sb, showing the levels of interest for the present Doppler shift attenuation method lifetime analysis.

stopped peak. In the analysis of the line shapes, corrections for the finite solid angle as well as for the finite-energy resolution of the detector were considered; the latter was determined from the photopeak response to a set of standard radioactive sources, and was accounted for by a Gaussian with smooth exponential tails on both sides.

The computer code performs a least-squares fit of the line shape by treating the level lifetime as a variable parameter, and could handle complex feeding patterns. In our case the feeding intensities of the levels under study were taken into account according to the decay scheme of Ref. [2]; the relevant level scheme considered in the present analysis is shown in Fig. 2. Thus, in the case of the 1937.2 and 3255.6 keV levels, only direct feeding was considered. In the case of the 2638 keV level, the feeding due to the isomeric $19/2^-$ state at 2792.6 keV was taken into account in addition to the direct feeding. For the 2517 keV level, in addition to the feeding due to the $19/2^-$ isomer, a long lifetime feeding from the second $19/2^-$ state at 2960.7 keV was included, due to the absence of Doppler broadening of the 443.8 keV transition from that level. It was also determined that the 374.5 and 428.0 keV transitions from the $11/2^+$ state at 1755.0 keV are not Doppler broadened, therefore the contribution of the feeding from the $2p$-$1h$ rotational band (Fig. 2) to the line shapes of the two $9/2^+$ states (1326.9 and 1380.6 keV) is only to their stopped peak component. Finally, for the 1098.6 keV level, the feeding from the two $9/2^+$ states and the long-time feeding due to the rotational band, as well as a small contribution from the 1504 keV level [13] were accounted for.

For the side-feeding times (τ_{sf}) of the investigated levels we have chosen values depending on the energy of the state and the position of the calculated entry region. The center of the entry region lies in our case at a relatively low energy, not exceeding 0.5–1.0 MeV above the states of interest. This leads to small values of the side-feeding times; in addition, we have assumed an increase in τ_{sf} with decreasing excitation energy of 0.03 ps/MeV. The values we have used for the side-feeding times (between 0.01 and 0.06 ps), which were not varied in the fitting procedure, are similar to those used for neighboring lighter [17] and heavier [18] nuclei. Actually, as the determined level lifetimes are of the order of 1 ps (see Table I), the influence of such feeding times on the final results and their errors is rather small.

The lifetime value of each level of interest was found by a best fit to the experimental line shapes of one of its decay-

TABLE I. Lifetimes of excited states in ^{115}Sb. J^π assignments in the second column are from Ref. [19].

E_{level} (keV)	J^π	τ [ps] Present	Ref. [13]	Others
770.4	$1/2^+$		$0.63^{+0.53}_{-0.21}$	
1071.7	$3/2^+$		$0.134^{+0.030}_{-0.020}$	
1098.6	$7/2^+$	0.83 ± 0.12	$0.46^{+0.45}_{-0.15}$	
1300.2	$11/2^-$			$(8.95\pm0.43)\times10^3$ [a]
1326.9	$9/2^+$	$1.75^{+0.30}_{-0.20}$		<7.2 [a]
1380.6	$9/2^+$	1.4 ± 0.4		<7.2 [a]
1504.2	$(3/2)^+$		0.153 ± 0.009	
1937.2		$1.3^{+0.5}_{-0.2}$		
2516.9	$15/2^-$	$0.6^{+0.3}_{-0.2}$		
2638.3	$15/2^-$	>3.0		
2796.2	$19/2^-$			$(2.29\pm0.04)\times10^5$ [1,2,3]
3255.6	$19/2^+$	$1.55^{+1.50}_{-0.70}$		
3659.7	$25/2^+$			$(5.92\pm0.29)\times10^3$ [a]

[a]Reference [2].
[b]Reference [3].
[c]Reference [12].

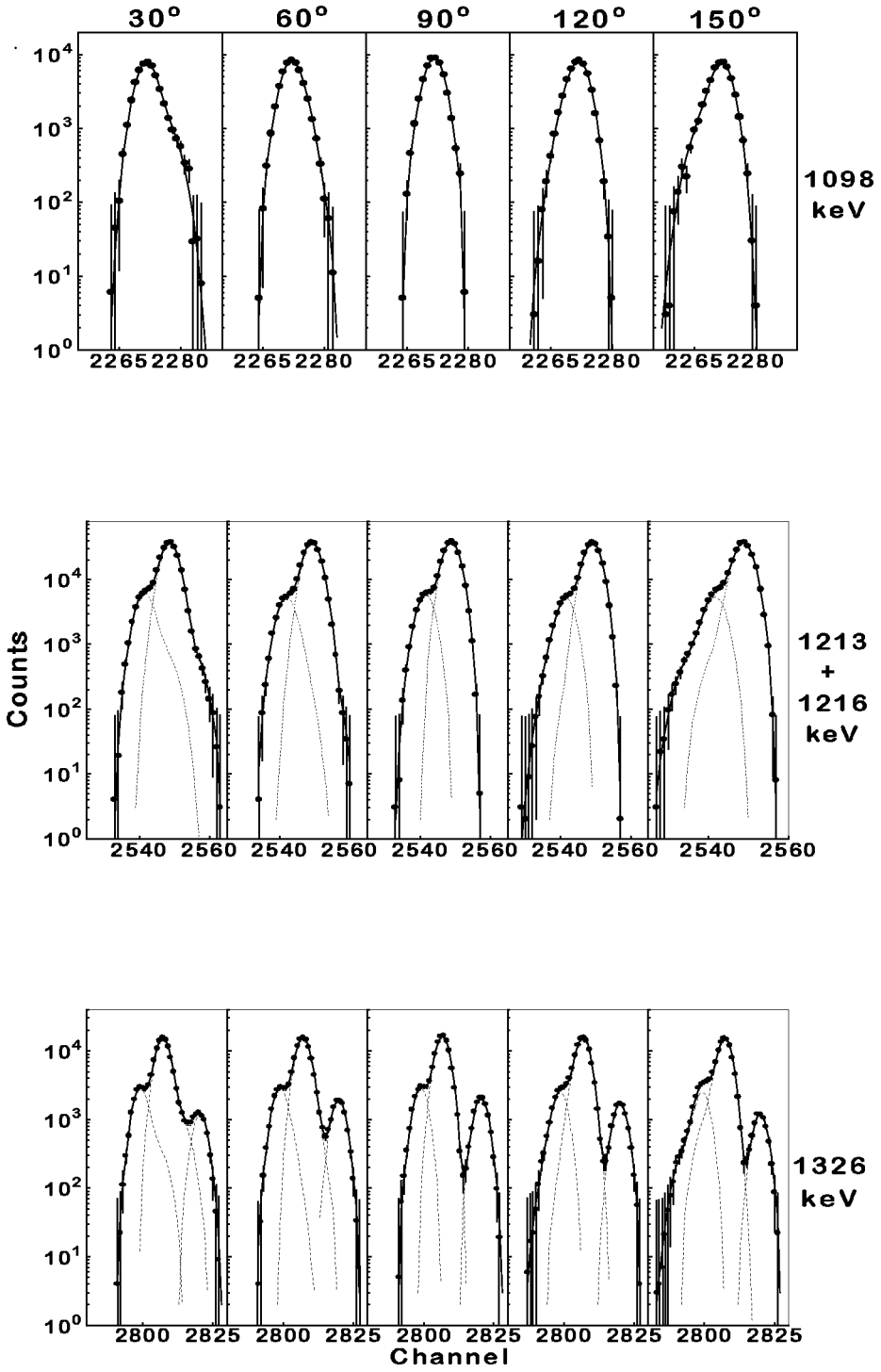

FIG. 3. Examples of DSA line shapes at different angles and their analysis for four transitions of ^{115}Sb (see Fig. 2). These are background subtracted portions of spectra (see the text). The continuous lines are the best Monte Carlo fits to the line shapes. The decomposition of these fits after the different components is also given by the dashed lines. Thus, the upper panels correspond to one single transition, the 1098.6 keV one (from the 1098.6 keV level). Those in the middle row illustrate the case of two overlapping transitions (1213.6 and 1216.7 keV from the levels at 1937.2 and 2516.9 keV, respectively) both with broadened line shapes. The lowest row of panels correspond to the more complex case of the 1326.9 keV transition (from the 1326.9 keV level), which partially overlaps with two other γ rays: 1332.0 keV (background line) on the right-hand side, which is not Doppler broadened, and 1322.9 keV on the left-hand side, which shows an effective lifetime of 1.5 ps. The lifetimes adopted from these analyses are given in Table I.

ing γ rays, which were obtained after performing a background subtraction from the region of interest. The background could be calculated as a polynomial up to the third order and was determined by a fit to neighboring portions of the spectrum which had no peaks; its typical values can be inferred from an inspection of Fig. 1. The computer code could take into account background peaks which overlap with the line shape; it also contained a procedure for analyzing two overlapping γ lines using for each one its lifetime as a parameter. As an illustration of the Doppler shift attenua-

TABLE II. Transition probabilities in ^{115}Sb. Branching ratios (I_γ) and mixing ratios (δ) are from Ref. [12].

E_{level} (keV)	E_γ (keV)	I_γ %	σL	δ	$B(E2)$ (W.u.)	$B(M1)\times 10^3$ (W.u.)
770.4	770.4	100	$E2$		146 ± 68	
1071.7	1071.7	100	$M1+E2$		129 ± 23 [a]	193 ± 35 [b]
1098.6	1098.6	100	$M1+E2$	$-3<\delta<-0.13$	8.7 ± 8.4	16 ± 13
1326.9	228.2	3.7(4)	$(M1+E2)$		650 ± 100 [a]	44 ± 7 [b]
	603.3	23(4)	$M1+E2$	0.12(4)	0.50 ± 0.31	15 ± 3
	1326.8	100(12)	$E2$		2.6 ± 0.4	
1380.6	281.9	4.4(4)	$(M1+E2)$		353 ± 109 [a]	37 ± 11 [b]
	656.9	31(1)	$M1+E2$	$-0.07(4)$	0.23 ± 0.21	20 ± 6
	1380.6	100(9)	$E2$		3.1 ± 1.3	
1504.0	405.4	24(9)	$(M1+E2)$		2915 ± 1200 [a]	630 ± 260 [b]
	780.4	21(6)	$(M1+E2)$		89 ± 30 [a]	71 ± 24 [b]
	1504.0	100(9)	$(M1+E2)$		15.4 ± 4.0 [a]	45 ± 12 [b]
1937.2	1213.6	100			6.8 ± 1.6 [a]	13 ± 3 [b]
2516.9	1216.7	100	$E2$		16.6 ± 6.4	
2638.3	322.2	23.7(20)	$M1+E2$	0.14(9)	<8.6 [a]	<6.0 [b]
	1338.2	100(10)	$E2$		<1.5	
3255.6	417.1	100(6)	$M1+E2$	0.116(6)	13.5 ± 7.7	230 ± 130
	797.9	47(9)	$E2$		18.2 ± 11.7	

[a]For pure $E2$ transition.

[b]For pure $M1$ transition.

tion analysis, Fig. 3 shows the line shapes of four transitions at the five measured angles. The lifetime values obtained from the present measurements as well as from other works are given in Table I. The present values represent weighted averages of the lifetimes determined separately at different angles. The errors include the statistical errors and a 20% uncertainty in the stopping powers used.

From Table I one can see that the lifetime value for the state at 1098.6 keV is, within errors, in reasonable agreement with the previous measurement. Also, the lifetimes for the states at 1326.9 and 1380.6 keV agree well with the previous limits of Ref. [2].

On the basis of the measured lifetimes, the reduced transition probabilities $B(\sigma L)$ were calculated and presented in Table II. The relative intensities of the γ-ray transitions and their multipole mixing ratios δ for mixed $M1/E2$ transitions were taken from [19]. Unfortunately, for some of the mixed transitions the mixing ratios are unknown. For such transitions the reduced probabilities were calculated as for pure $M1$ or $E2$ transition, respectively, corresponding to the extreme cases $\delta=0$ and $\delta=\infty$.

III. THEORETICAL CALCULATIONS AND DISCUSSION

In order to understand the energy levels of ^{115}Sb as well as their electromagnetic decay properties, we use the predictions of various nuclear models. We discuss first the low-lying positive parity levels. For this we have employed the interacting boson-fermion model (IBFM) [20] in its variant IBFM-1 which does not distinguish between neutrons and protons. The ^{115}Sb nucleus is described by coupling a fermion to a ^{114}Sn bosonic core. The Hamiltonian of these calculations is described in detail in Ref. [13]. The odd fermion is allowed to occupy all four positive-parity valence orbitals of the 50-82 shell ($2d_{5/2}$, $1g_{7/2}$, $3s_{1/2}$, and $2d_{3/2}$), whose energies have been chosen according to Ref. [21]. We have taken only the quadrupole-quadrupole term for the boson-fermion interaction, with a strength parameter $\Gamma_0=0.25$ MeV, which was determined such as to obtain a reasonable description of the positions of the lowest excited levels. The programs ODDA and PBEM [24] were used to calculate the energy levels and the electromagnetic transition probabilities, respectively. The electromagnetic transition operators used ''standard'' effective charges and gyromagnetic factors. For the effective boson charge we have taken a value of 0.1 eb—as determined from the $B(E2;2_1^+\rightarrow 0_1^+)$ value of the core [22] and for the fermion effective charge we chose also 0.1 eb (since the fermion is of ''particle'' type). For the gyromagnetic ratios the values used were $g_l=1$, $g_s=0.7g_\pi$, and an effective boson gyromagnetic ratio of -0.08 nm—as deduced from the magnetic factor of the 2_1^+ state of the core [23].

A comparison of the results of these calculations with the experimental level scheme is shown in Fig. 4, where correspondences between the experimental and calculated levels are indicated. The composition of the wave functions of some selected levels is presented in Table III. One can see that the dominant components are due to the $d_{5/2}$ and $g_{7/2}$ orbitals, whereas the $s_{1/2}$ and $d_{3/2}$ orbitals do not play an important role in the structure of the low-lying states. The dominant components are $\pi d_{5/2}\otimes 0_1^+$ for the $5/2_1$ ground state, and $\pi g_{7/2}\otimes 0_1^+$ for the $7/2_1$ state at 723.6 keV. For the upper states, one can recognize structures of multiplets originating from the coupling of the $d_{5/2}$ and $g_{7/2}$ protons to the quadrupole excitations of the core. Thus, the calculated

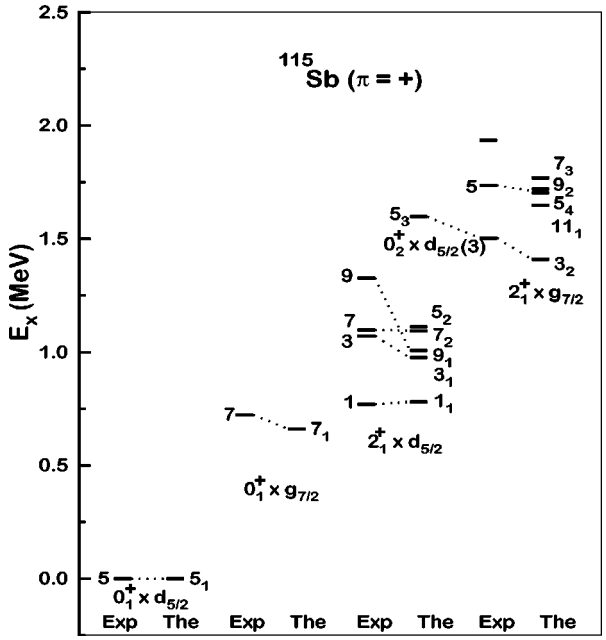

FIG. 4. Comparison between the experimental level scheme and the one calculated with the IBFM for the positive parity levels of ^{115}Sb. The levels are labeled by twice the value of their spin and are grouped according to their dominating configuration. The dotted lines indicate the assignments of the theoretical levels to the experimental ones (see the text). The two (tentative) assignments for the $E_x = 1504$ keV level are discussed in detail in the text. The level at $E_x = 1937$ keV probably belongs to the multiplet $2_1^+ \otimes g_{7/2}$ (see text and Table I).

states assigned to the experimental ones at 770.4 keV ($1/2_1^+$), 1071.7 keV ($3/2_2^+$), 1098.6 keV ($7/2_2^+$), and 1326.9 keV ($9/2_1^+$), respectively, belong to the multiplet $\pi d_{5/2} \otimes 2_1^+$ (the $5/2_2^+$ state was not identified experimentally). The upper states 1736.3 keV ($5/2^+$) and 1937.2 (no spin assignment) seem to belong to the multiplet $\pi g_{7/2} \otimes 2_1^+$: they were assigned to the calculated states $5/2_4^+$ and possibly one of the $7/2_3^+$, $9/2_2^+$ or $11/2_1^+$ states, respectively. For the state at 1504.2 keV [with $J^\pi = (3/2)^+$] we discuss, tentatively, two assignments: $3/2_2^+$, belonging to the above multiplet, or $5/2_3^+$, having the main configuration $\pi d_{5/2} \otimes 0_2^+$. These assignments will be discussed below on the basis of the electromagnetic decay data. We remark that the calculated level energies are in reasonable agreement with the experimental ones, except for the $9/2_1^+$ state at 1326.9 keV, which may be displaced due to its significant mixing with the other $9/2^+$ state at 1380.6 keV which originates from proton excitations of the core (as discussed below).

TABLE III. Wave functions of some low-lying states of ^{115}Sb, calculated by IBFM-1. The numbers represent the contributions (in percents) of each of the specified orbitals.

J^π	$s_{1/2}$	$d_{3/2}$	$d_{5/2}$	$g_{7/2}$
$1/2_1^+$	8.6	1.3	89.5	0.6
$3/2_1^+$	1.3	6.2	83.6	8.9
$3/2_2^+$	1.1	14.4	18.5	66.0
$5/2_1^+$	0.9	0.3	98.2	0.6
$5/2_2^+$	1.6	0.3	97.3	0.8
$5/2_3^+$	3.9	1.8	87.8	6.5
$5/2_4^+$	2.2	1.0	45.7	51.1
$7/2_1^+$	0.1	2.1	8.2	89.6
$7/2_2^+$	0.2	0.3	90.6	8.9
$7/2_3^+$	0.4	4.2	9.3	86.1
$9/2_1^+$	1.5	0.4	97.4	0.7
$9/2_2^+$	0.1	0.9	17.0	82.0
$11/2_1^+$	0.1	3.4	5.8	90.7

Table IV gives a comparison of the available experimental branchings and reduced transition probabilities with the calculated ones. One can see that the IBFM calculations provide, in general, a reasonable description of the electromagnetic decay properties of the low-lying states. In particular, these calculations reproduce the single-particle nature of the $7/2_1^+$ state. For some transitions, the $B(\sigma L)$ values also agree quite well, however, in a few cases the experimental $B(E2)$ values appear to be very large. The first case is that of the $1/2_1^+ \rightarrow 5/2_1^+$ transition (770.4 keV); it is possible that the lifetime of the $1/2^+$ state [13] has a much larger error, which should be expected for a very low-recoil experiment and a low $F(\tau)$ value. The second case is that of some transitions from the 1504 keV state. As it is given as a $(3/2)^+$ state [19] our first tentative assignment is the $3/2_2^+$ state. In this case, the strongest branch of this state, towards the $5/2_1^+$ state, is correctly reproduced by the calculations, but there are difficulties with the other branches; indeed, the experimental $B(E2)$ values of its decays towards the $7/2_2^+$ and $7/2_1^+$ states, which are pure $E2$ transitions, would be much too large (for the transition towards the $7/2_2^+$ state this is the situation even if the lifetime of this state [13] or the respective branch were wrong by a factor of, say, 5). In Ref. [13] it was stated that this situation could be due to a possible different spin assignment for this state. Another possibility would be that the 405.6 keV transition [which shows the too large $B(E2)$ value] is an unknown mixed ($M1/E2$) transition that does not belong to this state, but this is unlikely. Another possible assignment for this state, also tentative, is $5/2_3^+$, and this does not contradict the $\ell = 2$ transfer assignment in the (^{3}He,d) reaction [19]. In this case, the three measured branches of this state are also the main calculated ones, although their values are not reproduced in detail. A mixed $M1/E2$ character of all these three branches would lead to a much better agreement with the calculated B values (Table IV). Thus, a $5/2^+$ assignment to the 1504 keV state would appear more plausible. Since, however, we have no decisive arguments in favor of one of the two assignments discussed above, we indicate in Fig. 4 both of them, as tentative. The assignment of the state at 1736.3 keV as the $5/2_4^+$ calculated level is justified not only by a good description of its energy, but also by the fact that the calculations predict that it decays predominantly towards the $7/2_1^+$ state, as observed experimentally. For the 1937.0 keV state, one can see that the measured properties agree reasonably well with three possible assignments (to states from the second multiplet discussed above): in all three cases the theory predicts that the branching towards the $7/2_1^+$ state (which is the only one observed for this state) is by far the largest. However, we cannot prefer any of these assignments, so that we do not

TABLE IV. Comparison of $B(\sigma L)$ values provided by the IBFM-1 calculation with the experimental values.

E_{level} (keV)	J_i^π	J_f^π	E_γ (keV)	$I_\gamma(\%)$ Calc.	$I_\gamma(\%)$ Expt.	$B(E2)$ (W.u.) Calc.	$B(E2)$ (W.u.) Expt.	$B(M1)\times10^3$ (W.u.) Calc.	$B(M1)\times10^3$ (W.u.) Expt.
723.5	$7/2_1^+$	$5/2_1^+$	723.5	100	100	0.82		1.8	
770.4	$1/2_1^+$	$5/2_1^+$	770.4	100	100	11.6	146 ± 68		
1071.7	$3/2_1^+$	$1/2_1^+$	301.3	5.2	0	0.45		600	
		$7/2_1^+$	348.1	1.6×10^{-3}	0	0.76			
		$5/2_1^+$	1071.7	100	100	12.4	129 ± 23 [a]	234	193 ± 35 [b]
1098.6	$7/2_2^+$	$3/2_1^+$	26.9	10^{-10}	0	0.005			
		$7/2_1^+$	375.0	0.1	0	0.113		1.5	
		$5/2_1^+$	1098.6	100	100	13.9	8.7 ± 8.4 [c]	43	16 ± 13 [c]
1326.9	$9/2_1^+$	$7/2_2^+$	228.3	5.2	3.7(4)	0.175	647 ± 98 [a]	330	44 ± 7 [b]
		$7/2_1^+$	603.3	21.4	23(4)	8×10^{-4}	0.50 ± 0.31	73	15 ± 3
		$5/2_1^+$	1326.9	100	100(12)	14.0	2.6 ± 0.4		
1504.0 [d]	$3/2_2^+$	$7/2_2^+$	405.4	0.002	24(9)	0.15	2915 ± 1200		
		$3/2_1^+$	432.3	1.9	0	0.088		25	
		$1/2_1^+$	733.6	29.2	0	0.3		80	
		$7/2_1^+$	780.4	3.2	21(6)	9.1	89 ± 30		
		$5/2_1^+$	1504.0	100	100(9)	1.85	15.4 ± 4.0 [a]	26	45 ± 12 [b]
	$5/2_3^+$	$7/2_2^+$	405.4	64.1	24(9)	1.0	2915 ± 1200 [a]	116	630 ± 260 [b]
		$3/2_1^+$	432.3	18.4	0	4.2		27	
		$7/2_1^+$	780.4	100	21(6)	3.0	89 ± 30 [a]	23	71 ± 24 [b]
		$5/2_1^+$	1504.0	34.0	100	0.4	15.4 ± 4.0 [a]	0.1	45 ± 12 [b]
1937.0 [e]	$9/2_2^+$	$7/2_1^+$	1213.6	100	100	14.9	6.8 ± 1.6 [a]	21	13 ± 3 [b]
	$7/2_3^+$	$7/2_1^+$	1213.4	100	100	12.4	6.8 ± 1.6 [a]	8.3	13 ± 3 [b]
	$11/2_1^+$	$7/2_1^+$	1213.4	100	100	14.9	6.8 ± 1.6		

[a]For pure $E2$.

[b]For pure $M1$.

[c]For τ from [13]: $B(E2)=15.2\pm15.2$ W.u., $B(M1)\times10^3=28.1\pm26.9$ W.u.

[d]Two possible assignments for this state (see the text for discussion).

[e]Different spin assignments for the state at 1937.0 keV; the other (calculated) branches possible in each case are not given since they are practically insignificant.

draw a definite conclusion about the spin of this state.

We consider now in detail the decay of the two $9/2^+$ states at 1326.9 and 1380.6 keV. We may assume that the $9/2_1^+$ state at 1326.9 keV is basically the result of coupling a $d_{5/2}$ proton with the 2_1^+ state of ^{114}Sn, as presented above. On the other hand, the $9/2_2^+$ state at 1380.6 keV may be the result of a transition of a $g_{9/2}$ proton to a higher orbital [25]. This leads to the formation of an intruder, $2p$-$1h$ configuration with moderate deformation ($\varepsilon\approx0.2$) and a rotational band built on this state (see Fig. 2). The relatively low-energy of the band head was explained by shell model calculations with a residual p-n interaction taken into account [25]. The two $9/2^+$ states are closely spaced and therefore one can expect that they mix with each other. The presence of the $9/2_1^+\rightarrow7/2_2^+$ and $9/2_2^+\rightarrow7/2_2^+$ transitions and of the $11/2_1^+\rightarrow9/2_1^+$ and $11/2_1^+\rightarrow9/2_2^+$ transitions (by $11/2_1^+$ we mean the known state, at 1755 keV, from the rotational band) point to a possible mixing of two states which have different intrinsic configurations. The simple IBFM calculations that we have performed account only for the states resulting by coupling single-particle degrees of freedom to the states of the core (described in our case as an anharmonic vibrator). These calculations do not describe the occurrence of the second $9/2^+$ state at about the same excitation energy. For this reason, we have analyzed the decay properties of these two $9/2^+$ states on the basis of the previous calculations [2] in the frame of the cluster-vibrational model [26]. These calculations implied in a unified manner the coupling of both single-particle states and the $2p$-$1h$ cluster with one-, two- or three-phonon states of the Sn core. Table V presents the results of these calculations compared to the experimental ones. The good agreement suggests the suitability of such a model for the description of the mixing of the two states in ^{115}Sb: one resulting from the coupling of a one $d_{5/2}$ quasiparticle to the 2_1^+ state of the core, and the other from a proton excitation of the core across the $Z=50$ shell.

The lowest $15/2^-$ and $19/2^-$ states in the odd antimony isotopes are usually interpreted as $\pi d_{5/2}\otimes5^-$ and $\pi d_{5/2}\otimes7^-$, respectively. This interpretation is based on the systematics of the $19/2^-$-$15/2^-$ energy spacings in the Sb isotopes and of 7^--5^- spacings in the Sn cores [27]. The observed $B(E2;19/2^-\rightarrow15/2^-)$ value in ^{115}Sb is enhanced with respect to the $B(E2;7^-\rightarrow5^-)$ value in ^{114}Sn, and this enhancement is explained by the admixtures of $\pi h_{11/2}\otimes2_1^+$ and $\pi h_{11/2}\otimes4_1^+$ components to the $15/2^-$ and $19/2^-$ states,

TABLE V. Calculated (Ref. [2]) and experimental transition probabilities from the two $9/2^+$ states.

E_γ	I_γ(%)		δ		$B(E2)$ (W.u.)		$B(M1)\times10^2$ (W.u.)	
(keV)	Calc.	Expt.	Calc.	Expt.	Calc.	Expt.	Calc.	Expt.
1327	70	79(10)			5.0	2.6 ± 0.4		
603	30	18(3)	0.001	0.12(4)	1.5×10^{-4}	0.50 ± 0.31	3.9	1.5 ± 0.3
1381	75	74(5)			1.3	3.1 ± 1.3		
657	25	23(5)	-0.05	$-0.07(4)$	1.2×10^{-2}	0.23 ± 0.21	0.34	2.0 ± 0.6

respectively. From the measured τ value of the $15/2^-$ state at 2516.9 keV it follows $B(E2;15/2^-\rightarrow11/2^-)=16.4\pm6.4$ W.u., which coincides with the value $B(E2;2_1^+\rightarrow0_1^+)=16.8\pm5.8$ W.u. in ^{114}Sn [28], a fact which indicates the presence of a large collective component in the $15/2^-$ state.

IV. CONCLUSIONS

The lifetimes of six excited states of ^{115}Sb have been measured by the Doppler shift attenuation method in the $(\alpha,2n\gamma)$ reaction. The structure of the low-lying states in this nucleus was interpreted in the frame of the multishell interacting boson-fermion model. The lifetime data extend the knowledge about the level structure at low and medium energies and allowed a more precise assignment of the configurations involved in these states. They also characterize better the mixing between the single particle and the $2p$-$1h$ intruder configurations. In some cases, the present data could be described only qualitatively, but a detailed analysis will be possible when more accurate spin and parity assignments, as well as mixing ratios for the mixed $M1/E2$ transitions will become available.

ACKNOWLEDGMENT

This work was partly supported by research grant No. 3225/1997 from the Romanian Academy of Sciences.

[1] R. Kamermans, T. J. Ketel, and H. Verheul, Z. Phys. A **279**, 99 (1976).
[2] J. Bron, W. H. A. Hesselink, H. Bedet, H. Verheul, and G. Van den Berghe, Nucl. Phys. **A279**, 365 (1977).
[3] R. E. Shroy, A. K. Gaigalas, G. Schatz, and D. B. Fossan, Phys. Rev. C **19**, 1324 (1979).
[4] M. E. J. Wigmans, R. J. Heynis, P. M. A. Vander Kam, and H. Verheul, Phys. Rev. C **14**, 243 (1976).
[5] C.-B. Moon, S. J. Chae, J. H. Ha, T. Komatsubara, J. Lu, T. Hayakawa, and K. Furuno, Z. Phys. A **352**, 245 (1995).
[6] R. S. Chakrawarthy and R. G. Pillay, Phys. Rev. C **54**, 2319 (1996).
[7] V. P. Janzen, D. R. LaFosse, H. Schnare, D. B. Fossan, A. Galindo-Uribarri, J. R. Hughes, S. M. Mullins, E. S. Paul, L. Persson, S. Pilotte, D. C. Radford, I. Ragnarsson, P. Vaska, J. C. Waddington, R. Wadsworth, D. Ward, J. Wilson, and R. Wyss, Phys. Rev. Lett. **72**, 1160 (1994).
[8] D. R. LaFosse, D. B. Fossan, J. R. Hughes, Y. Liang, H. Schnare, P. Vaska, M. P. Waring, J.y. Zhang, R. M. Clark, R. Wadsworth, S. A. Forbes, and E. S. Paul, Phys. Rev. C **50**, 1819 (1994).
[9] V. P. Janzen, H. R. Andrews, B. Haas, D. C. Radford, D. Ward, A. Omar, D. Prevost, M. Sawicki, P. Unrau, J. C. Waddington, T. E. Drake, A. Galindo-Uribarri, and R. Wyss, Phys. Rev. Lett. **70**, 1065 (1993).
[10] D. R. LaFosse, D. B. Fossan, J. R. Hughes, Y. Liang, M. P. Waring, and J.y. Zhang, Phys. Rev. Lett. **69**, 1332 (1992).
[11] D. R. LaFosse, D. B. Fossan, J. R. Hughes, Y. Liang, H. Schnare, P. Vaska, M. P. Waring, and J.y. Zhang, Phys. Rev. C **56**, 760 (1997).
[12] J. Konijn, T. J. Ketel, and H. Verheul, Z. Phys. A **289**, 287 (1979).
[13] D. Bucurescu, I. Căta-Danil, G. Ilaş, M. Ivaşcu, L. Stroe, and C. A. Ur, Phys. Rev. C **52**, 616 (1995).
[14] I. Kh. Lemberg and A. A. Pasternak, *Modern Methods of Nuclear Spectroscopy* (Nauka, Leningrad, 1985).
[15] J. Lindhard, V. Nielsen, and M. Scharff, K. Dan. Vidensk. Selsk. Mat. Fys. Medd. **36**, 10 (1968).
[16] I. Kh. Lemberg and A. A. Pasternak, Nucl. Instrum. Methods **140**, 71 (1977).
[17] L. Funke, J. Döring, P. Kemnitz, E. Will, G. Winter, A. Johnson, L. Hildingsson, and Th. Lindblad, Nucl. Phys. **A455**, 206 (1986).
[18] P. J. Smith, D. J. Unwin, A. Kirvan, D. J. G. Love, A. H. Nelsson, P. J. Nolan, D. M. Todd, and P. J. Twinn, J. Phys. G **11**, 1271 (1985).
[19] J. Blachot and G. Marguier, Nucl. Data Sheets **67**, 1 (1992).
[20] F. Iachello and O. Scholten, Phys. Rev. Lett. **43**, 679 (1979).
[21] B. S. Reehal and R. A. Sorensen, Phys. Rev. C **2**, 819 (1970).
[22] S. Raman, C. W. Nestor, S. Kahane, and K. H. Bhatt, At. Data Nucl. Data Tables **42**, 1 (1989).
[23] P. Raghavan, At. Data Nucl. Data Tables **42**, 189 (1989).
[24] O. Scholten, computer codes ODDA and PBEM, KVI Internal Report No. 252 (1982).
[25] K. Heyde, J. Ryckebuch, M. Waroquier, and J. L. Wood, Nucl. Phys. **A484**, 275 (1988).
[26] G. Van den Berghe and E. Degrieck, Z. Phys. **262**, 25 (1973).
[27] L. K. Kostov, W. Andrejtscheff, L. G. Kostova, A. Dewald, G. Bohm, K. O. Zell, P. von Brentano, H. Prade, J. Doring, and R. Schwengner, Z. Phys. A **337**, 407 (1990).
[28] I. N. Vishnevsky, G. B. Krygin, Yu. N. Lobach, V. E. Mitroshin, A. A. Pasternak, and V. V. Trishin, Ukr. Phys. J. **36**, 1132 (1991).